

## Creation and nature of optical centres in diamond for single-photon emission—overview and critical remarks

This article has been downloaded from IOPscience. Please scroll down to see the full text article.

2011 New J. Phys. 13 035024

(<http://iopscience.iop.org/1367-2630/13/3/035024>)

View [the table of contents for this issue](#), or go to the [journal homepage](#) for more

Download details:

IP Address: 134.76.223.56

The article was downloaded on 21/06/2012 at 11:42

Please note that [terms and conditions apply](#).

## Creation and nature of optical centres in diamond for single-photon emission—overview and critical remarks

Sébastien Pezzagna<sup>1,2,5</sup>, Detlef Rogalla<sup>1</sup>, Dominik Wildanger<sup>3</sup>, Jan Meijer<sup>1</sup> and Alexander Zaitsev<sup>1,4</sup>

<sup>1</sup> RUBION, Ruhr-Universität Bochum, Universitätsstraße 150, 44780 Bochum, Germany

<sup>2</sup> Research Department IS<sup>3</sup>/HTM, Ruhr-Universität Bochum, 44780 Bochum, Germany

<sup>3</sup> Department of NanoBiophotonics, Max Planck Institute for Biophysical Chemistry, Am Faßberg 11, 37077 Göttingen, Germany

<sup>4</sup> The College of Staten Island, City University of New York, 2800 Victory Blvd, Staten Island, NY 10314, USA

E-mail: [sebastien.pezzagna@rub.de](mailto:sebastien.pezzagna@rub.de)

*New Journal of Physics* **13** (2011) 035024 (27pp)

Received 20 October 2010

Published 29 March 2011

Online at <http://www.njp.org/>

doi:10.1088/1367-2630/13/3/035024

**Abstract.** A huge variety of optical colour centres can be found in diamond, emitting in its whole wide transparency range. Although several of these centres have been demonstrated as single-photon emitters, none of them meets all of the requirements of an ideal single-photon source. In this view, we discuss the properties of prominent optical centres, such as the nitrogen vacancy, the silicon vacancy or the so-called NE8 centre, as well as recently found centres ascribed to defects containing Ni, Si, Cr and Xe. Besides suitable intrinsic properties, it is necessary for practical applications that optical centres can be created artificially on demand. Of all known methods, only ion implantation allows for the most controlled creation of such defect centres. In this paper, we discuss how nanoscalability, that is, the nanometre placement and the deterministic creation of optical centres, can, could or cannot be achieved by the available ion implantation techniques. A fine analysis of individual optical centres is now possible, thanks to the recently developed subdiffraction optical microscopy methods.

<sup>5</sup> Author to whom any correspondence should be addressed.

**Contents**

|  |           |
|--|-----------|
| <b>1. Introduction</b>   | <b>2</b>  |
| <b>2. General concepts of ion implantation</b>   | <b>3</b>  |
| 2.1. Factors limiting spatial resolution . . . . .   | 3         |
| 2.2. Control of the ion fluence . . . . .  | 5         |
| 2.3. Surface preparation . . . . .   | 5         |
| 2.4. Annealing . . . . .   | 6         |
| <b>3. Ion implantation at nanoscale</b>  | <b>7</b>  |
| 3.1. Heavy-ion, high-energy microbeam . . . . .  | 8         |
| 3.2. Resist techniques using electron beam lithography . . . . .                               | 9         |
| 3.3. Low-energy nanoimplanter . . . . .  | 9         |
| 3.4. Deterministic ion implantation techniques . . . . .                                       | 10        |
| 3.5. High-resolution optical inspection . . . . .  | 12        |
| <b>4. Optical centres in diamond for single-photon emission</b>                                | <b>13</b> |
| 4.1. NV <sup>-</sup> centre . . . . .  | 14        |
| 4.2. SiV centre . . . . .  | 15        |
| 4.3. NE8 centre . . . . .  | 15        |
| 4.4. Other impurity-related centres . . . . .  | 18        |
| 4.5. Intrinsic optical centres . . . . .   | 18        |
| 4.6. Optical centres for fibre optics . . . . .  | 20        |
| <b>5. Application of optical centres in diamond single photon light-emitting diodes (LEDs)</b> | <b>20</b> |
| <b>6. Conclusion and outlook</b>   | <b>23</b> |
| <b>Acknowledgments</b>   | <b>23</b> |
| <b>References</b>  | <b>24</b> |

**1. Introduction**

Single-photon quantum information processing is a hot area in today's physics. One of the main challenges to be met on the way of practical realization of single-photon informatics is the development of a reliable single-photon source working at room temperature [1]–[4]. It is also of importance that the spectral and temporal parameters of the emission of this source comply with the requirements of optical transmission systems [5]. The qualities of a good single-photon source are long-time stability, low noise emission at room temperature, narrow spectral range of emission, working spectral range matching the spectral ranges of fibre optics and single-photon detectors and, last but not least, nanoscalability [6, 7], which could allow us to manipulate it at a precision of a few nanometres. Considering all of these requirements together, one sees that the point optical centres in solids made by ion implantation or embedded in nanocrystals are the best choice, provided that these centres can be engineered with high precision and efficiency. By now, a number of optical centres in diamond have been demonstrated as stable single-photon emitters working at room temperature. Among them, the nitrogen-vacancy (NV) centre, the silicon-vacancy (SiV) centre and the so-called NE8 centre are the most prominent ones. Although diamond was not really chosen among other optical materials for the role of a single-photon emitter matrix, one may understand that it occurred

because of the unique optical properties of diamond, which surpass by far all other materials. Indeed, perfect diamond has the widest spectral range of transparency from deep ultraviolet through to far infrared. An enormous number of optically active structural defects (optical centres) may emit photons in this spectral range [8]. There are hardly any examples of optical centres in diamond that could be destroyed via optical excitation or emission. The temperature stability of photoemission of many optical centres is unprecedented, attaining temperatures over 500 °C. Optical centres in diamond can be created individually by single-ion implantation, which makes them unique in terms of nanopositioning. The use of these optical centres is not restricted to single-photon sources: their high-emission efficiency, combined with other suitable properties, finds important applications, for example, in biolabelling or quantum information processing, as already demonstrated with NV centres. Although nanometer positioning is not necessary for single-photon sources designed as generators of trains of single photons in quantum communication lines, the fabrication of quantum registers based on single-photon sources does require precise positioning with an accuracy of a few nanometres.

The first part of this paper will review the basic concepts of ion implantation related to the production of single optical centres. Then, the different ion implantation techniques will be presented and their performance and limitations will be discussed in terms of spatial resolution and control of the number of implanted ions. The third part will give an overview of the impurity-related and intrinsic optical centres in diamond, which can be used for single-photon emission. Finally, a possible way of realization of a room-temperature electrically driven single-photon source based on a diamond p–i–n light-emitting diode will be discussed.

## 2. General concepts of ion implantation

The ion implantation technique is widely used for a large number of applications in research and industry. Recently, ion implantation has also been shown as a unique method of controllable creation of single optical centres based on isolated point defects in solids. Demanding requirements for the control of the atomic structure of individual defects and the precision of their positioning push the ion implantation technique to its limits, and even require the development of new ion implantation concepts.

### 2.1. Factors limiting spatial resolution

Whatever the focusing capabilities of an ion implantation set-up, the spatial resolution of the size and positioning of the ion-implanted volume is limited by the straggling of ions propagating in the implanted substrate. The straggling (deviation of ions from their mean straight line propagation) occurs due to the multiple collisions of the moving ions with the atoms of the substrate. The straggling results in a broadening of the ion-implanted volume, the size of which depends on the nature of the implanted ions, the ion energy, the target material and the crystallographic direction of the implantation. Quantitatively, the ion straggling is defined as the square root of the variance of the ion distribution. It can be decomposed into longitudinal (along the implantation direction) and transverse (perpendicular to the implantation direction) straggling. However, the values of both longitudinal and transverse straggling have comparable magnitudes and therefore one may refer to one straggling as a measure of broadening or increase of the ion-implanted volume. Straggling increases with the ion energy. For nitrogen ions implanted into diamond with energies of a few keV, the straggling is in the range of a

few nanometres. As the ion energy increases to the MeV range, the ion straggling becomes greater than 100 nm (simulated by the SRIM code [9]). Since the ion straggling is an inherent and unavoidable effect of ion implantation, high-energy ion implantation cannot be used for the impurity doping with spatial accuracy in the nanometre range. Instead, low-energy ions have to be used for nanoscale ion implantation. In this case, however, the implanted ions come to rest in close proximity to the surface (at a depth of a few nanometres) and the state of the surface may considerably modify the properties of the implants.

Another important effect of the ion implantation into crystal substrates is ion channelling—a deeper penetration of the ions propagating along low-index crystallographic axes and planes [10, 11]. Measurements show that the channelled ions may penetrate much deeper into the substrate and that they result in considerably less damage to the lattice [7, 12]. For a given channelling direction, ion species and sample temperature, the channelling occurs above a minimum ion energy  $E_{\min}$  and within a critical angle  $\psi_{\text{crit}}$ . The dependence of  $\psi_{\text{crit}}$  on the ion kinetic energy  $E$  presents a maximum  $\psi_{\text{crit}}^{\text{max}}$  and behaves as

$$\psi_{\text{crit}} \propto E^{-1/2} \text{ for the high-energy part and } \psi_{\text{crit}} \rightarrow 0 \text{ when } E \rightarrow E_{\min}. \quad (1)$$

In practice, the part of the implanted ions undergoing channelling strongly depends on many parameters of the ion implantation procedure and the state of the substrate, and it is therefore hardly predictable. The channelling effect, especially for the ion energies below 100 keV, is a serious problem that has to be taken into account. Note that channelling cannot be simulated with SRIM. In order to suppress the channelling effect, the angle between the ion beam and the crystallographic directions of the substrate must be properly controlled. Usually, for cubic crystals like Si, Ge and diamond, an angle of  $7^\circ$  with respect to any of the main crystallographic axes has been found to be the most ‘non-channelling’ direction of ion implantation [13]. Thus, in practice, in order to avoid extensive channelling, ion implantation is usually performed at an angle of  $7^\circ$  with respect to the normal to the substrate surface, provided that the substrate is cut along one of the main crystallographic planes. Another method used for suppression of channelling is the deposition of a thin amorphous layer on the substrate surface. In this case, while travelling through the amorphous layer, the ions lose their initial direction of propagation and enter the underlying crystal substrate in random directions.

Implantation of ions always causes damage to the crystal lattice of any substrate (radiation defects) along the ion tracks. In the case of diamond, the radiation defects are mainly single vacancies, interstitial carbon atoms and their simple complexes. In order to restore the damaged crystal lattice, the ion-implanted diamonds are usually annealed at high temperatures [14, 15]. The diffusion of the implanted species during annealing may occur and contribute to uncertainty of the final position of the implanted species. Fortunately in diamond, the diffusion of any atoms (save for hydrogen), including nitrogen, is extremely slow and the high-temperature treatments are not expected to significantly affect the as-implanted resolution. However, vacancies are mobile [16, 17], and it is their diffusion that allows for the formation of defects like the NV centres, since nitrogen atoms are efficient traps for vacancies [18].

The charging up of the substrate surface during ion implantation is an additional serious hurdle for precise ion implantation. Since diamond is an excellent insulator, charging up may lead to dramatic losses in the resolution because of electrostatic deviation of the ions from their initial trajectories. This effect is especially pronounced for implantations with low energies. Besides the loss of resolution, the charging may considerably slow down the ions approaching the substrate. The charging may easily change the electric potential of the substrate by ten

thousands of volts and therefore make the implantation impossible. However, this problem of charging can be avoided by exposing the implanted substrate to an electron shower or by covering it with a thin conductive layer.

## 2.2. Control of the ion fluence

The ion fluence (number of implanted ions per unit area), along with the ion species and the ion energy, is a main parameter of ion implantation. The control of the ion fluence is a critical issue in the creation of single-photon emitters. Firstly, an important parameter of optical centres like the yield or creation efficiency (ratio between created centres and implanted ions) can be determined accurately only if the ion fluence is properly controlled. Secondly, the scalable creation of single optical centres requires that the number of implanted ions is controlled precisely. In practice, in order to cover the large range of ion fluences (from the implantation of single ions to the implantation of regions with high density of ions), different ion implantation techniques and therefore different ways to control the ion fluence have to be used. The best control is achieved in the ideal case of a deterministic ion implantation (see section 3.4); either the source delivers a predetermined number of ions or the system is capable of counting the impact ions on the substrate. However, with the standard implantation techniques presented in section 3, the current measurement and the control of the implantation time are the main sources of error. This is especially true in the case of very low fluences for which the ion current has to be reduced to a few pA and/or the implantation time to a few seconds or fraction of second. Measurement of pA ion currents is not easy and could be affected by wrong calibration or inductive charging up of the wires. Moreover, for very short-time implantations, the closing time of the measuring cup or the time of reaction of the beam blanking and scanning systems become significant.

Finally, the efficiency of formation of some optical centres may depend on the density of the ion beam (ion flux). This may occur when the defect cascades created by individual ions overlap, or when the substrate is heated up by the intense ion beam. Both mechanisms depend on the ion species and the ion energy. However, for diamond, with its very good thermal conductance, the increase in temperature during implantation is small.

## 2.3. Surface preparation

The surface preparation is an important issue for the creation of single-photon emitters in diamond. The quality of the sample surface is especially critical for shallow optical centres. A perfect cleanness of the surface ensures that low-energy ions are properly implanted. Before ion implantation, the sample is usually ultrasonically cleaned in acetone and isopropanol. The residual adsorbed layer is then expected to be not thicker than 1 nm and its effect is insignificant for the ions with energy of a few keV. For example, the energy loss of a nitrogen ion with energy below 5 keV in water is about  $150 \text{ eV nm}^{-1}$  (calculated with SRIM). In order to reduce the water adsorption, the diamond surface can be terminated with hydrogen. It has been shown that the hydrogen-termination makes the diamond surface very stable and hydrophobic [19, 20].

A critical issue for the creation of shallow optical centres is the surface roughness. A surface with a roughness of 10 nm (a standard for commercially available diamond samples) is not appropriate for an implantation to a depth of a few nm. The roughness enlarges the surface area and therefore strengthens the influence of the surface. Additionally, the crystal quality under a rough surface is low. The experience with NV centres shows that some of their properties

are influenced by the proximity of the surface, depending on whether they are in the bulk or shallow (like in nanodiamonds). It has been shown recently that for shallow implanted samples, the surface plays a significant role in the charge state of NV centres. In particular, negatively charged NV centres are mainly produced with an oxygen-terminated surface [21]–[23].

#### 2.4. Annealing

After ion implantation, the samples have to be annealed. Annealing is necessary for three reasons. Firstly, the implanted impurity atoms have to be placed in the lattice positions, where they work as optically active defects. Secondly, most of the impurity-related optically active defects comprise vacancies and/or interstitial carbon atoms. Therefore, annealing is necessary to make the intrinsic defects mobile and to bring them to the impurity atoms. Thirdly, annealing reduces the overall crystal damage caused by the ion bombardment and restores the crystal lattice. The crystal damage results in a strong non-radiative recombination of charge carriers in diamond. Thus, the restoration of crystal lattice around an optically active defect is imperative to achieve its efficient luminescence.

Atomic transformations in diamond during annealing are very complex processes and they have not been fully studied and understood yet. Generally, it is believed that single self-interstitial atoms and their simple aggregates may become mobile in diamond lattice at very low temperatures and they completely anneal out by a temperature of 400 °C. Single vacancies are more stable defects and they start to move at a temperature of 600 °C. The complete annealing of vacancies can be achieved only at a temperature of 1000 °C.

The mobility of impurity atoms in diamond at high temperature is still an open question too. However, it is known that the long-range diffusion of any impurity, save for hydrogen, is extremely slow and it can be neglected at temperatures of up to 2000 °C. However, a short-range migration within a few interatomic distances in the vicinity of other lattice defects might be very probable and this short-range migration may influence the formation of the impurity-related defects considerably. Thus, the defect structure formed during ion implantation and even the initial impurity-defect structure of diamond sample are very important for the formation of optically active defects. As an example, we consider the behaviour of the NV centres formed and processed in diamond in different ways. An annealing at 800 °C is required to well activate NV centres in nitrogen-implanted diamond. However, a higher temperature of 1200 °C seems to be necessary to achieve better results, like a longer  $T_2$  coherence time of the electron spin associated with an  $NV^-$  centre [24]. Figure 1 shows how different the annealing behaviour of NV centres in the nitrogen-implanted diamonds treated in different ways may be.

It is seen that in diamonds subjected to ordinary low-dose nitrogen ion implantation, NV centres start to form at a temperature of 600 °C, when vacancies become mobile. In these diamonds, NV defects are stable to a temperature of 1400 °C and at higher temperatures they aggregate, producing more complex defects like H3 (N-V-N or V-N-N-V complex) and N3 ( $N_3V$  complex). In contrast, the temperature of aggregation of NV defects in diamonds implanted with high dose of nitrogen and subsequently subjected to an annealing under high pressure is considerably lower – 1200 °C only. On the other hand, in diamonds implanted simultaneously with nitrogen and helium, NV centres become very temperature stable and they do not reveal reduction in intensity at temperatures up to 1600 °C. The same effect of the temperature stabilization of NV centres has also been observed in diamonds after dual implantation with  $N^+$  and  $Xe^+$  ions [8]. This effect of stabilization of optical centres by implantation of noble gases

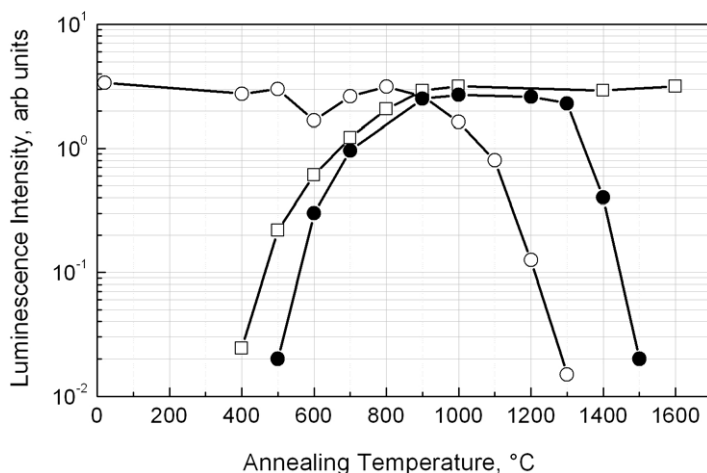


**Figure 1.** Change of luminescence intensity of the  $NV^0$  centre in diamonds implanted with nitrogen and treated in different ways: (●) low nitrogen-type IIa diamond implanted with 300 keV  $N^+$  ions at a dose of  $10^{13} \text{ cm}^{-2}$ ; (□) low-nitrogen-type IIa diamond after dual implantation with 300 keV  $N^+$  ions at a dose of  $3 \times 10^{15} \text{ cm}^{-2}$  and 100 keV  $He^+$  ions at the same dose; (○)-type IIa diamond implanted with 300 keV  $N^+$  ions at a dose of  $10^{16} \text{ cm}^{-2}$  and subsequently annealed at 1600 °C under pressure of 60 kbar [8].

is not unique for diamond. A similar effect is known for optical centres in silicon [25]. Although this effect has not been fully understood yet, we assume that noble gas atoms, because of great covalent radius, may strongly distort the surrounding crystal lattice and serve as stoppers for the diffusion of defects and impurities.

Many other impurities, like nitrogen, form optically active centres in ion-implanted diamond only after annealing at temperatures above 600 °C. Most of these centres are rather temperature stable and do not anneal out at temperatures up to 1500 °C. However, the optimized annealing procedures are still a matter of research and may differ from one optical centre to another.

A specific feature of annealing of diamond is the temperature-induced surface graphitization. It is well known that the diamond surface, when heated at temperatures above 900 °C, becomes graphitized. The rate of this graphitization and the thickness of the graphitized layer strongly depend on the temperature, duration of the annealing and presence of oxygen in the annealing atmosphere. Annealing in a vacuum of  $10^{-7}$  mbar (oxygen content in residual atmosphere is about  $10^9 \text{ cm}^{-3}$ ) at a temperature of 1400 °C for 2 hours may result in a nanometre-thick graphitic layer, whereas annealing in argon (oxygen content even in commercially available argon of ultra pure grade is about  $10^{14} \text{ cm}^{-3}$ ) at the same temperature–time parameters could produce a hundred nanometre-thick graphitic layer. Thus, the graphitization effect becomes especially important for low-energy ion implantation, when the implantation depth is only a few nanometres.

### 3. Ion implantation at nanoscale

Although the introduction of some impurities is possible during the diamond growth, ion implantation is the only way to produce optical centres in a controlled way aiming at

nanoscalability. Here, we discuss different ion implantation techniques, which have been successfully used for the production of NV centres via implantation of nitrogen. Although all of these methods are applicable for any ion species, we will focus our discussion on the nitrogen-related NV centres, which offer the best possibilities in terms of characterization. Indeed, the NV centres in diamond have proved to be an almost ideal test bed for high-resolution microscopy (single NV centres can be resolved optically with a few nm resolution [26]). In addition, the NV centres have been widely studied in the last decades as single-photon source, basic element for a room-temperature quantum computer [27]–[29], nanoscale magnetic sensor [30]–[32] and biological marker [33, 34].

Of more than five hundred known optical centres of diamond, only a few have been artificially produced by ion implantation (see section 4) so far, and a wide field is still to be explored. Below, the different techniques are discussed in terms of their capabilities to create single optical centres. Two main characteristics are considered: the spatial resolution and the control of the number of implanted ions.

In conventional set-ups like accelerators with focused ion beams, the control of the number of implanted ions can be achieved only statistically described by Poisson law. This is a very serious disadvantage for the applications where nanoscalability is required. A precise control of the number of implanted ions can eventually be achieved by postdetection of single-ion impacts. However, this is possible only for highly charged ions or high implantation energies. In order to solve this problem, deterministic single ion sources are being developed, based on ion traps that are further modified to extract and accelerate single ions, one at a time.

### 3.1. Heavy-ion, high-energy microbeam

Microbeam systems are able to focus the ion beams delivered by an accelerator down to a few hundreds of nanometres. The spot size depends on the ion beam current, the optical quality of the ion lenses and the mechanical stability of the whole set-up. A large number of proton microbeams of 3 MeV energy are available. Most of them are optimized for proton-induced x-ray emission (PIXE) application and use magnetic quadrupole lenses. The focusing power of such systems is about 3 MeV a.m.u., which is not high enough to focus heavier ions like nitrogen. Only a few quadrupole systems worldwide are able to focus heavy ions so far. However, the problem of quadrupole systems is the large number of free parameters. As a result, the change in the ion species leads to the change in the ion pathway, and this requires a new alignment. Besides this problem, the magnetic remanence of the quadrupole lenses makes any change in the ion species and/or the ion kinetic energy very difficult. To resolve these problems, a single-lens system based on a superconductive 14 T solenoid without any ferromagnetic core has been developed in Bochum (figure 2). This system achieves a focusing power of 100 MeV a.m.u. and is capable of focusing any ions in the energy range from 500 keV to more than 20 MeV [35].

This system allows a fast and easy change in ion species and/or ion energy, which can be done within 30 min. The chromatic aberration is comparable to quadrupole systems; however, the spherical aberration is about one order of magnitude smaller. In order to perform ion implantation of large structures in a short time, the system is equipped with an ion projection set-up [36]. For single-ion implantation, apertures of a few micrometres in diameter are used. These microapertures reduce the intensity of the ion beam down to a few hundreds ions per second. The number of the passing ions may be measured by direct irradiation of a surface barrier detector. Unfortunately, the system is not able to count *in-situ* single ions during the

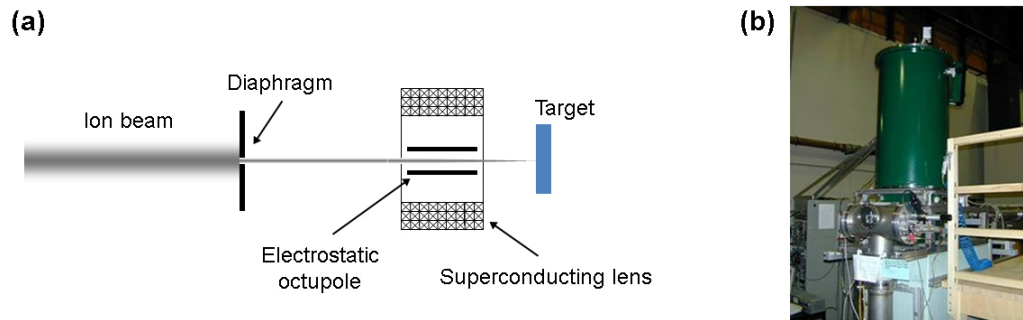


**Figure 2.** (a) Schematic diagram of the ion microbeam set-up. The ion beam delivered by the accelerator is formed by an aperture and focused with the superconductive solenoid lens on the target. An in-lens electrostatic octupole is used for correction of the lens aberration and for scanning the ion beam. (b) Photo of the microbeam system currently used in the Ruhr-University Bochum. The green cylinder is the helium cryostat cooling the 14 T superconducting magnet.

implantation of the sample, and therefore only statistical predictions are possible. The expected number of implanted ions per irradiated spot is set by tuning the frequency of the scanning unit. The least spot size of this system is about 300 nm [37], which is about the least size of the ion-implanted area when using high-energy ions. Indeed, the broadening of the ion-implanted area in diamond due to straggling may exceed 100 nm for ions with a few MeV energy.

In the purpose of limiting the ion straggling, low-energy ions have to be implanted. However, focusing a low-energy ion beam to spot sizes below 10 nm is highly challenging. Although modern focused ion beam (FIB) set-ups using liquid metal gallium sources nowadays reach single-digit nanometre beam sizes, this is impossible for a FIB using a gas source such as nitrogen (which is not a point-like source), mainly due to chromatic aberration. Two different concepts have been successful in providing high-resolution implantation (a few tens of nm) of nitrogen in diamond: either using a photoresist mask or without any mask.

### 3.2. Resist techniques using electron beam lithography

In this first approach, photoresist is spin coated on diamond and further patterned by electron beam lithography [7, 38]. A compromise has to be found between the resist thickness and the desired aperture size: the resist must be thick enough to stop the impinging ions but thin enough to allow the development of small holes. Within a 200 nm-thick PMMA layer (which stops N ions up to 20 keV), apertures with diameters down to 30 nm could be demonstrated. Thanks to a relatively fast e-beam writing process, this permits the fabrication of arrays of shallow optical centres at a chip-scale.

### 3.3. Low-energy nanoimplanter

In the second and maskless approach, a system combining a low-energy nitrogen beam and a pierced atomic force microscopy (AFM) tip has been developed [6, 39]. The nitrogen beam is prefocused on the backside of the AFM tip that has a nanohole in it and the resolution of the set-up thus directly depends on the size of the nanohole (figure 3(a)). Figure 3(b) shows such

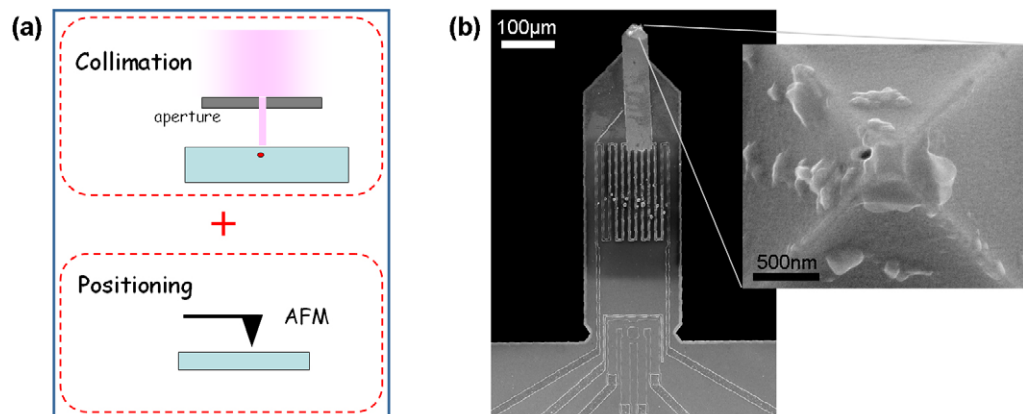


**Figure 3.** (a) Schematic diagram of the low-energy nanoimplanter setup that combines collimation and positioning of an ion beam within the pierced tip of an AFM microscope. (b) SEM image of the AFM piezoresistive cantilever. The inset shows the pyramidal hollow tip in which a hole has been drilled close to its summit by a focused ion beam.

a piezoresistive tip in which a nanohole is drilled by FIB milling (inset). After the primary FIB milling, the size of the aperture can be reduced using subsequent exposure of the tip to high-dose ion irradiation [40]. The ion beam current can be measured either with a Faraday cup (high current beams) or with an electron multiplier (low-current beams for implantation of single ions). Manipulation with the tip permits a nanometer precise placement of the aperture over the sample surface providing in this way the ion beam writing of two-dimensional nanostructures. This technique of pierced AFM tip has shown the highest resolution (20 nm) for the creation of NV centres [6].

As the single-ion implantation techniques are evolving rapidly, it seems that it will be possible soon to reliably implant single atoms in diamond with nanometer accuracy. The control of the number of implanted ions still remains a great challenge of the described nanoimplanter. So far, it is possible to perform only a statistical implantation of individual ions. However, even at its present state, we expect that the capability of the nanoimplanter to work with different ions and its high spatial accuracy of implantation will allow us to complete very challenging tasks; for instance, to place an individual optical centre in a photonic cavity.

### 3.4. Deterministic ion implantation techniques

Deterministic implantation (implantation of exact number of ions) of low-energy ions could be realized in two ways: either using a detection system capable of counting the number of ion impacts onto the sample or using a single-ion source that delivers a predetermined number of ions. Both approaches have already been realized. In the first approach, the pulse of secondary electrons produced by ion impacts is measured. This technique, however, is possible only for ion energies of more than 20 keV or for highly charged ions [41]. For implantation in Si, it is also possible to detect the single-ion implantation events by measuring the pulses of the electrical current produced by the generation of electron–hole pairs [42]. Unfortunately, this technique is hard to implement for diamond.

The second approach, starting from an ion trap and shooting one ion out of it, allows a fully deterministic implantation of countable single ions [43]. Another advantage of the method is that

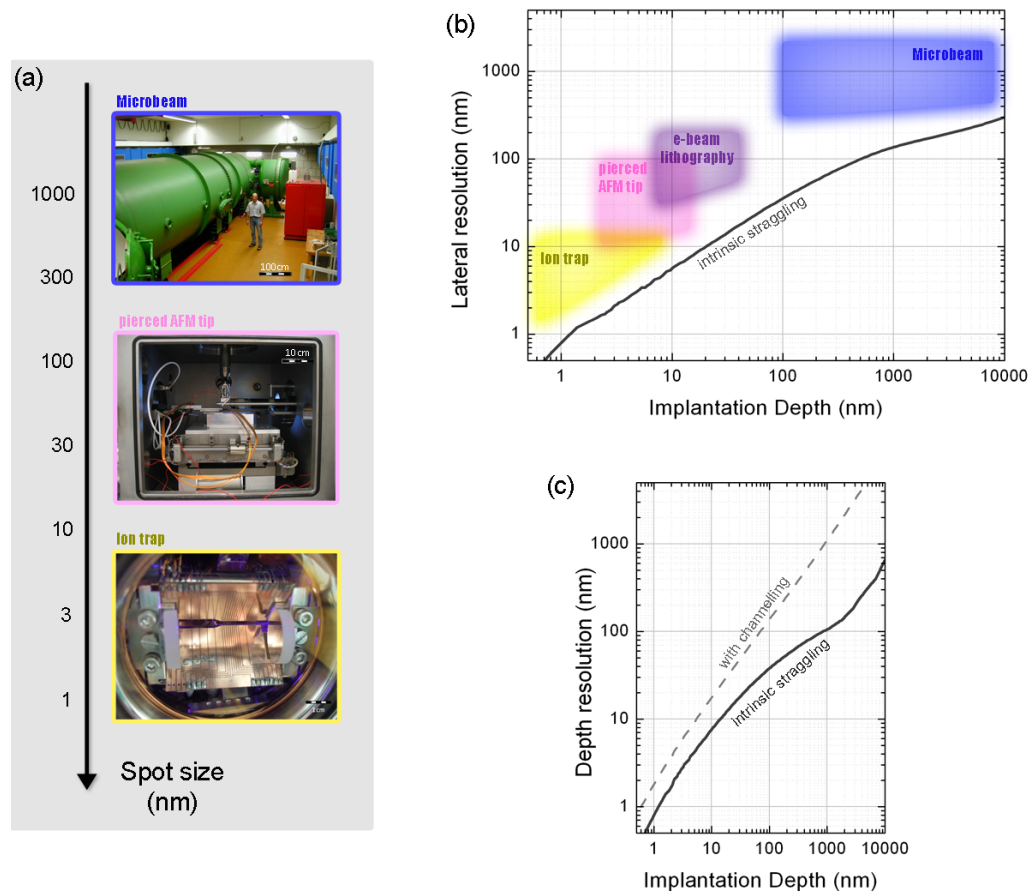


**Figure 4.** (a) Spot size obtained for the different implantation techniques. 300 nm for the microbeam and 20 nm for the pierced AFM tip have already been demonstrated. For the ion trap (photo, courtesy of K Singer), the expected resolution is in the nm regime. (b) Plot of the lateral broadening as a function of implantation depth. The corresponding ranges of the implantation techniques are also shown. (c) Depth broadening due to intrinsic straggling. The dashed line shows the resulting additional broadening in case of 50% of the ions channelling twice deeper.

an ion starts with very low chromatic aberration. If the ions are further cooled to the motional ground state (Heisenberg limit), this type of source would therefore be the ultimate ion source for low-energy ion implantation [44]. In such a case, calculations predict a lateral resolution of 0.1 nm and the first experimental tests are very promising [45]. Obviously, implanting one ion at a time makes it the most time demanding of all techniques. However, it is the only one ensuring deterministic ion implantation and it should be possible to increase the rates of single-ion implantation up to the kHz regime.

In figure 4(a), the resolution capabilities of the previously described ion implantation methods are summarized. The resolution limit due to intrinsic lateral straggling is plotted in figure 4(b) as a function of the implantation depth (i.e. as a function of the ion energy) for nitrogen ions in diamond. Figure 4(c) shows the longitudinal straggling as well as the resulting depth broadening if channelling takes place.

### 3.5. High-resolution optical inspection

The luminescence of optical centres can be easily imaged using a fluorescence microscope operating in confocal or wide-field mode. Like in any optical far-field technique, the imaging is limited by diffraction and therefore—depending on the wavelength employed—the centres placed closer than a certain distance cannot be resolved individually. In recent years, techniques have been developed to overcome the diffraction barrier for fluorescent markers. They are all based on switching the fluorescent system between a bright/signalling and a dark/non-signalling state in combination with time sequential read-out from diffraction-limited volumes. In particular, different approaches of the RESOLFT (REversible Saturable Optical Fluorescence Transitions) concept [46], namely STED [47] (Stimulated Emission Depletion), GSD [48]–[50] (Ground State Depletion) via dark-state population or saturation [51] and spin-RESOLFT [52], have been employed to image the NV colour centre in diamond with resolutions down to 5 nm [26]. Although all these techniques rely on the same concept, they differ in detail.

The STED technique utilizes stimulated emission as the switching process. The excitation and STED beams are superimposed and focused into the sample. The focal intensity distribution of the STED beam is engineered to possess an intensity minimum at its centre. Therefore, the markers at the very centre of the beam are not affected and show spontaneous fluorescence, whereas at a certain distance from the centre (which only depends on the intensity of the STED beam) the local STED intensity is high enough to ensure that only stimulated emission but no spontaneous fluorescence can occur. Since only the spontaneous fluorescence is detected, a marker undergoing stimulated emission is non-signalling or dark. The size of the central unsuppressed area of the STED beam, where the emission of optical centres may occur, determines the resolution of the STED microscope. This size depends not only on the wavelength of the STED beam, but, and this is very important, on the STED beam intensity: the higher the intensity, the smaller the unsuppressed area, which can be as small as a few nanometres. Thus, scanning the STED beam over the sample, one can resolve optical centres at very short distances.

The GSD method is based on the depopulation of the ground state of optical centres. Two different implementations have been shown so far: (i) pumping the fluorescent system in a metastable non-fluorescent dark state and subsequent probing of the centres that remained in the bright state [50]; (ii) fluorescence saturation for the centres showing constant emission intensity when excited above a certain threshold (saturating centres). If the intensity distribution of the excitation beam is shaped like a doughnut, a colour centre at the middle of this doughnut is not excited. Given a high-enough intensity of the excitation light, all centres located even a tiny distance away from the centre of the doughnut emit with maximal intensity. Thus, scanning the sample with such a beam and detecting the luminescence response results in a negative high-resolution image [51]. In case of the NV centre, STED is the most promising technique. It is as fast as the confocal imaging, has an excellent signal-to-noise ratio and provides the highest resolution so far [6]. Figure 5 shows the STED imaging of a pattern of shallow NV centres created by 5 keV nitrogen ion implantation through a pierced AFM tip.

Although saturation-based GSD microscopy may provide similar resolution to that of STED, it suffers from a much greater signal-to-noise ratio. The enhanced noise of the GSD imaging results from the unavoidable excitation of all centres, which are located in the diffraction-limited volume. This drawback is especially detrimental to samples with a high density of optical centres. In the spin-RESOLFT method, a high level of noise may be even more pronounced because of the low imaging contrast characteristic of this technique.

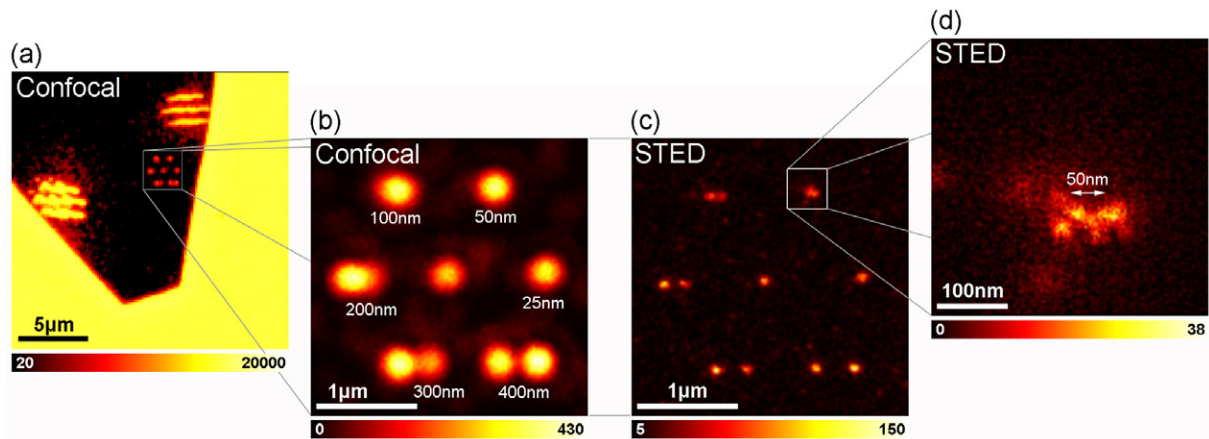


**Figure 5.** Imaging NV centres created by implantation through an AFM tip pierced with three holes. (a) Confocal scan revealing the implanted pattern through each of the holes, all clearly visible within the dark area covered by the tip during implantation. The intensity scale of (a) is logarithmic. (b) Confocal scan of the pattern created through a hole of  $\sim 75$  nm diameter. (c) STED scan of the same pattern. (d) STED scan of the double spot separated by 50 nm. Experimental details: the images were acquired by scanning the area of implantation with a self-made STED microscope employing pulsed (8 MHz) excitation and stimulated emission at 532 and 775 nm, respectively. In order to achieve a resolution of approximately 10 nm, an STED power of 1 W is applied to the sample. Considering a pulse length of 3 ns, this gives a focal intensity of  $11 \text{ GW cm}^{-2}$ . The excitation laser features a pulse length of only 100 ps. The excitation power was measured to be  $125 \mu\text{W}$  and thus a focal intensity of  $3.7 \text{ MW cm}^{-2}$  was achieved. The spontaneous fluorescence was collected with an avalanche photodiode. The detection window is centred on 700 nm with a width of 60 nm. From the fluorescence intensity it can be concluded that the spots visible in (d) stem from single-NV centres.

An advantage of the GSD method is its applicability to optical centres emitting in narrow spectral ranges, e.g. optical centres emitting preferentially in zero-phonon lines (ZPL). Spectrally narrow emission is a very valuable quality for a single-photon source. However, imaging of such centres with STED microscopy might be a challenging task, since the narrow spectral range of emission makes it difficult to separate the photons created by spontaneous luminescence from those generated by stimulated emission. If such centres provide metastable dark states, the usage of the dark-state-based GSD method may be advisable.

#### 4. Optical centres in diamond for single-photon emission

Although several optically active defects in diamond have been demonstrated as single-photon emitters, neither of them meets all of the requirements of a good single-photon source, which are high structural stability, high luminescence efficiency at room temperature, narrow spectral range of emission and short luminescence lifetime. So far, the following optical centres in diamond have been studied as single-photon sources:  $\text{NV}^-$  (637 nm), SiV (736 nm), NE8

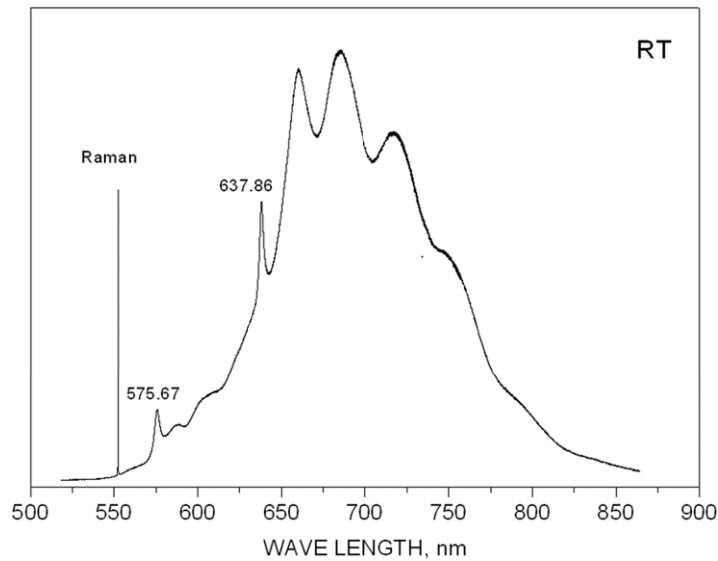


**Figure 6.** Photoluminescence spectrum of the  $\text{NV}^-$  centre in a single-crystal CVD diamond film excited at room temperature with 514 nm Ar-laser line. The centre exhibits a pronounced ZPL at about 638 nm accompanied by multiple phonon replica. A minor line at 575.67 nm is ZPL of the  $\text{NV}^0$  centre.

(794 nm), and a few optical centres of unknown nature emitting in a spectral range from 730 to 770 nm.

#### 4.1. $\text{NV}^-$ centre

The  $\text{NV}^-$  centre with ZPL at 638 nm is the most studied one (e.g. [53]). Its room-temperature luminescence spectrum is shown in figure 6. The  $\text{NV}^-$  centre has been used for the first demonstrations of single-photon communication, single shot readout of nuclear spin and quantum register with coupled electron spins [29, 54, 55].

The  $\text{NV}^-$  centre is optically very stable and has high quantum efficiency at room temperature. The  $\text{NV}^-$  centre is one of the best high-temperature emitters in diamond (figure 8). However, it has a serious drawback: it has a strong electron–phonon interaction and as a result a very broad emission spectrum ranging from 600 to 850 nm. The contribution of the zero-phonon line in the spectrum (Debye–Waller factor) at room temperature amounts to only a few per cent. Besides the strong electron–phonon interaction, a disadvantage of the  $\text{NV}^-$  centre is its long lifetime that could amount to 25 ns [56]. The long lifetime does not allow the  $\text{NV}^-$  centre to emit single photons at a high repetition rate. These disadvantages may preclude the  $\text{NV}^-$  centre from use in quantum communication systems.

Individual  $\text{NV}^-$  centres can be created in diamond nanocrystals by CVD growth techniques. However, the reproducibility of the CVD fabrication of diamond nanocrystals containing single optical centres is very low. As seen in section 3, individual  $\text{NV}^-$  centres can also be made in diamond by single nitrogen ion implantation and, in principle, can be positioned with a spatial precision of a few nanometres [6]. However, since the NV centre is a complex of nitrogen atom and vacancy, the efficiency of its creation by ion implantation is strongly affected by the NV interaction and because of this may be very low, especially at low fluences and low

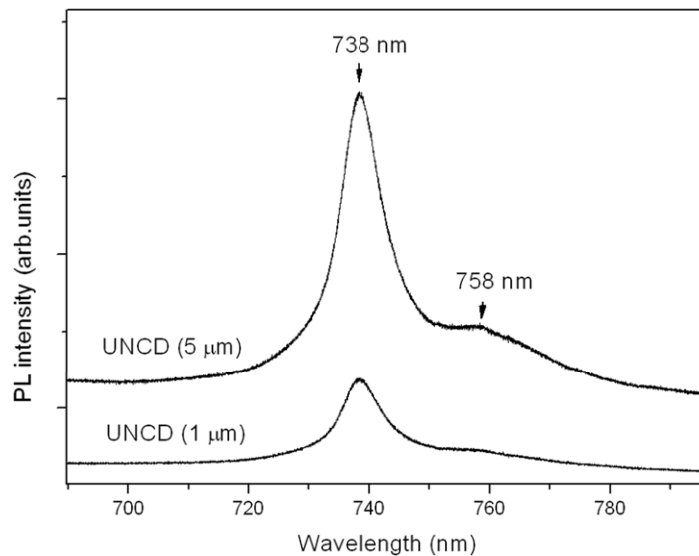


**Figure 7.** Photoluminescence spectra of SiV centre in nanodiamond recorded at RT [60]. Copyright Wiley-VCH Verlag GmbH & Co. KGaA. Reproduced with permission.

energies. It has been shown in [57] that the yield (measured after nitrogen ion implantation and subsequent annealing at 800 °C for 2 h) is very low, amounting to only 1% for N ions at keV energies, whereas it can reach 50% when the implantation has been carried out at MeV energies. For nanoscalability, high creation efficiency is a critical issue. The yield of the NV<sup>-</sup> centres made by ion implantation can be improved by creating more vacancies around the implanted N atoms [58], or by charging the NV defects [21]–[23], [59].

#### 4.2. SiV centre

The SiV centre is another diamond optical centre that is promising for single-photon communication. The advantages of the SiV centre are its much narrower emission spectrum than that of the NV<sup>-</sup> centre (figure 7) and its much shorter lifetime of 1.2 ns [2]. At room temperature, the SiV centre emits mainly in its zero-phonon line at 738 nm, having a spectral width of about 10 nm.

SiV centres can be produced in diamonds by ion implantation [2]. Their emission efficiency is high and it remains high even when the centres are embedded in diamond nanocrystals [61]. Like the NV<sup>-</sup> centre, the SiV centre is a complex defect comprising an impurity atom and a vacancy and, consequently, the efficiency of the fabrication of SiV centres by implantation of individual Si ions may also be low. In addition, the SiV centre may reveal a noticeable temperature quenching of its luminescence intensity with a temperature increase from LNT to RT (figure 8). So the total luminescence intensity of the SiV centre may be 5 times weaker at RT than that recorded at LNT.

#### 4.3. NE8 centre

The NE8 (ZPL at 793 nm) centre has recently attracted a lot of attention because of its spectral and temporal parameters that seem more attractive for applications in fibre optics quantum

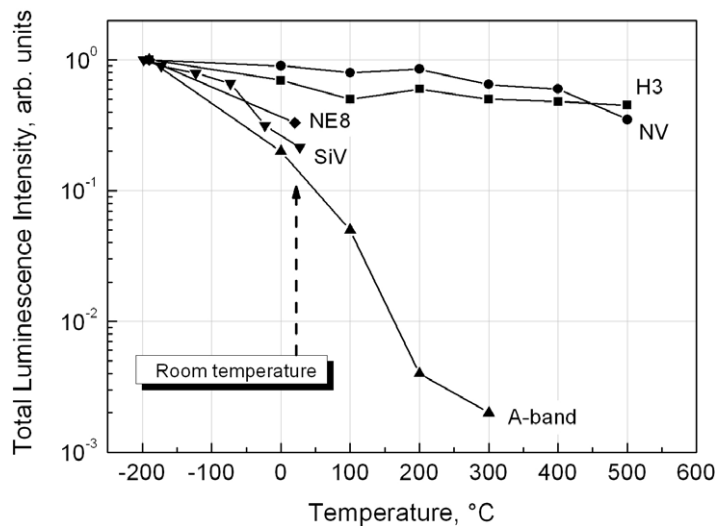


**Figure 8.** Temperature dependence of the luminescence intensity of some optical centres common for ion-implanted diamonds: the H3 centre (■), the NV<sup>0</sup>/NV<sup>-</sup> centres (●), the A-band (▲), the SiV centre (▼) and the NE8 centre (◆). NV and H3 centres are the most temperature stable.

communication systems than those of the NV<sup>-</sup> and SiV centres [62, 63]. Strong emission at room temperature, 2 ns short lifetime and seemingly narrow spectra emission range concentrated mainly in ZPL have been considered as the advantages of the NE8 centre.

However, a careful analysis of the vibronic spectrum of the NE8 centre recorded in a broad spectral range shows that the electron–phonon coupling at this centre is not really weak (figure 9(a)). At liquid nitrogen temperature, the Debye–Waller factor of the NE8 centre is about 0.04, and it decreases to 0.01 with a temperature increase to room temperature. These values are quite common for a vast majority of optical centres in diamond. Regarding the temperature stability, the NE8 centre reduces its total luminescence intensity about 3 times when diamond is heated from LNT to RT (figure 8). The temperature-induced reduction of the intensity of the ZPL is even greater (figure 9(b)).

There are some peculiarities of the electron–phonon interaction at the NE8 centre, which can be explained by its atomic structure comprising four nitrogen atoms and one nickel atom (4N + Ni). The analysis of the spectra in figure 9(a) and that presented in [64] allow us to isolate three vibronic features with energies of 34, 42 and 68 meV. A very weak second-order replica of these vibrations can be recognized as a hump at wavelengths from 850 to 890 nm. Since the density of phonon states of the diamond lattice has no features up to energies of 73 meV, all of the aforementioned vibrations can be ascribed to quasi-local modes of the NE8 centre. Following the model of quasilocal vibrations proposed in [65], we can estimate the mass of the impurity atoms involved in these vibrations. According to this model, the frequency  $\omega_R$  of the local vibration is given by the formula

$$\omega_R = \omega_D \sqrt{\frac{M_C}{3(nM_I - M_C)}}, \quad (2)$$

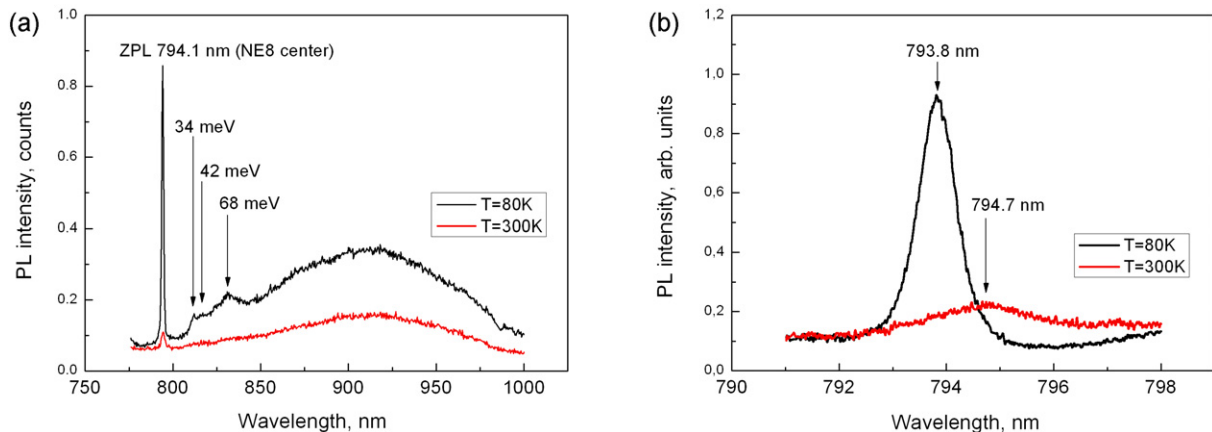


**Figure 9.** Photoluminescence spectra of the 793.6 nm Ni-related optical centre ascribed to NE8 paramagnetic centre recorded at liquid nitrogen (black curves) and room temperature (red curves). (a) Total spectrum of the NE8 centre showing its vibronic side-band. (b) Detailed spectra of zero-phonon line. Spectra are taken for a synthetic diamond (courtesy of A Yeliseyev).

where  $M_C$  and  $M_I$  are the masses of carbon atom and impurity atom, respectively, and  $\omega_D = 150$  meV is the Debye frequency of the diamond lattice. Although this formula was derived assuming the isotopic character of the impurity atom, it also describes satisfactorily the energies of quasi-local vibrations of many chemically different impurities in diamond [66, 67]. Assuming that the low-energy 34 meV vibration is driven by the motion of the whole  $4N + Ni$  cluster, the formula gives the energy for this vibration as 29.7 meV. This calculated energy is in reasonable agreement with the experimental value of 34 meV. The 42 meV vibration can be ascribed to the local vibration of the Ni atom alone and/or the cluster of four N atoms. Indeed, the calculations give the energy of local vibration of 44.2 meV for the Ni atom and 45.2 meV for four N atoms. Both values are also close to the experimental energy of 42 meV. The feature at 69 meV is most probably the second-order replica of the 33 meV vibration.

It is remarkable that the vibronic side-band of the NE8 centre does not have any features related to the optical phonons of the diamond lattice, which are commonly present in vibronic side-bands of many optical centres of diamond (e.g. see the 389 nm centre in [66]). The structureless broad band with a maximum at 920 nm is the result of the dominant interaction with low-energy acoustic phonons, which have no features in the spectrum of their density of states. Such a dominant interaction with long-wave acoustic phonons is characteristic of large multiatom defects.

Although the NE8 centre has attractive spectral parameters, there is one severe challenge about it. Namely, the NE8 centre could not be created in diamond by ion implantation so far. Assuming that the atomic structure of the NE8 centre is four nitrogen atoms surrounding one Ni atom, attempts have been made to synthesize  $4N + Ni$  defects by co-doping of diamond with nitrogen and nickel during the CVD growth and by dual  $N^+$  and  $Ni^+$  ion implantation [53, 68]. Nevertheless, no success has been achieved using any of these methods.

Another disadvantage of the NE8 centre as a single-photon source is its assumingly multilevel electronic structure, which, notwithstanding the short life time, considerably reduces the rate of the single-photon emission down to 0.1 MHz [3].

One more issue worth mentioning is the remarkably different wavelengths of ZPL of the NE8 centre ranging from 794 to 802 nm, as reported by different authors [5], [62]–[64], [69]. Such a great difference in the spectral position of the ZPL raises the question as to whether the same centre was being discussed. Since many optical centres with ZPLs close to 800 nm may be observed in diamond [8, 70], it could be that they have all been erroneously ascribed to the NE8 centre.

#### 4.4. Other impurity-related centres

Several other optical centres emitting at the wavelengths of 768, 746, 749, 764, 756 and 772 nm and ascribed to defects containing Ni, Si and Cr atoms have been reported as efficient single-photon emitters [4], [71]–[75]. These centres were found in diamond nanocrystals grown by the CVD method, or were made in bulk diamonds by ion implantation of the corresponding species. The atomic structure of these centres and even their atomic composition have not been established yet. However, the 768 nm centre has been tentatively ascribed to a complex containing Ni and Si atoms, the 746, 749, 764, 756 nm centres have been ascribed to Cr-containing defects, while the 772 nm centre might be a defect incorporating simultaneously Cr and Ni atoms. A great advantage of these centres is a short luminescence lifetime and a large Debye–Waller factor. These favourable parameters result in high-emission efficiency. For instance, the luminescence lifetime of the 749 nm Cr-related centre is about 1 ns, which makes it the most efficient single-photon emitter working in bulk diamond. However, the record of efficiency belongs to the 756 nm centre (in nanodiamond), which is the most efficient single-photon emitter reported so far: its single-photon emission rate is about  $3.2 \times 10^6$  counts  $s^{-1}$ .

A centre of unknown nature with ZPL at 734 nm is observed at room temperature in photoluminescence spectra of CVD diamond films [3]. This centre is believed to be a true two-energy-level system. The emission of the 734 nm centre occurs entirely in its ZPL. The centre has a very high Debye–Waller factor of 0.81. According to the spectrum presented in [3], the 734 nm centre does not reveal any vibrational replica in the energy range up to 140 meV. Thus, one may believe that the Debye–Waller factor of this centre could be even greater approaching the ultimate value of 1. Unfortunately, the lifetime of the 734 nm centre is rather long reaching 13.6 ns, which is comparable with that of the  $NV^-$  centre. However, the two-level energy structure makes the 734 nm centre much more efficient in terms of the rate of single-photon emission than the  $NV^-$  centre. Indeed, the experimentally measured single-photon emission rate of the 734 nm centre attains a value of 1.6 MHz.

#### 4.5. Intrinsic optical centres

So far, all but one luminescence centre in diamond demonstrated as single-photon emitters are impurity-related ones. The TR12 centre with ZPL at a wavelength of 471 nm (figure 10(a)) is the first intrinsic defect for which single-photon emission was shown too [76].

The TR12 centre appears to be an impractical single-photon emitter. Indeed, the efficiency of its formation even with high-energy ion irradiation is very low, amounting to only 0.1%. The TR12 centre has a developed vibrational side-band resulting in a small Debye–Waller factor of 0.1 even at low temperatures. That is, the emission of the centre is not monochromatic but occurs in a broad spectral range from 470 to almost 600 nm. However, an advantage of the TR12

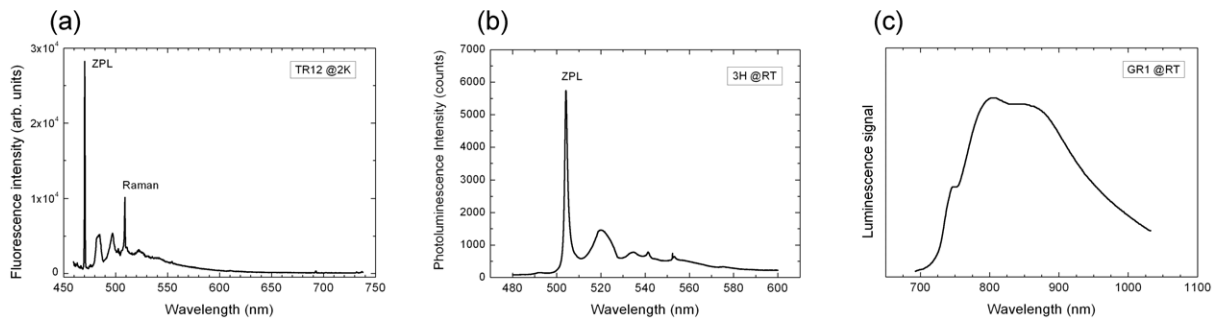


**Figure 10.** Fluorescence spectrum of a single TR12 centre at  $T = 2$  K. The ZPL at 470.5 nm belongs to the TR12 defect. The measured line width (full-width at half-maximum) is 0.14 nm (limited by spectrometer resolution). (b, c) PL spectra of the 3H and GR1 centres measured in irradiated natural diamonds at room temperature. (b) 3H centre after high-energy ion irradiation; (c) GR1 centre after electron irradiation [77].

centre is its relatively short fluorescence lifetime of 3.6 ns, what could be a prerequisite of high single-photon efficiency.

Besides the TR12 centre, there are two more prominent intrinsic optical centres in diamond, which could be considered as candidates for single-photon emitters. They are the GR1 centre (single vacancy) with ZPL at 742 nm (figure 10(c)) and the 3H centre (a vacancy-interstitial cluster) with ZPL at 504 nm (figure 10(b)). Although their single-emission capabilities have not been investigated yet, we can analyse optical parameters of these centres relevant to single-photon emission. Both the GR1 and 3H centres are readily created in diamond by any irradiation including high-energy electrons, neutrons and ions. For instance, the efficiency of generation of the GR1 centres in low nitrogen diamonds by 0.5 MeV electrons is about 100%, that is, every 0.5 MeV electron produces on average one active GR1 centre.

Spectra of the GR1 and 3H centres differ considerably in terms of electron–phonon coupling. Although both centres interact predominantly with acoustic phonons, the strength of the electron–phonon interaction is very strong for the GR1 centre, whereas it is weak for the 3H centre. The Debye–Waller factor for the emission of these centres at room temperature is about 0.01 (GR1) and about 0.3 (3H). That is, the emission of the 3H centre is much more monochromatic than that of the GR1 centre.

The luminescence decay time of the GR1 centre is rather short, ranging from 2 to 4 ns [78]. However, it was found that the true radiative lifetime of the GR1 centre may be much longer attaining 180 ns [8]. Thus, it is believed that the GR1 centre has a very strong non-radiative decay channel [79]. There are no data about the radiative lifetime of the 3H centre. However, it has been shown that the 3H centre, like the GR1, also has a strong non-radiative decay channel [80]. Usually, the 3H centre in ion-irradiated low-nitrogen diamonds has luminescence intensity comparable to that of the GR1 centre. Therefore, one can assume that the lifetime parameters for both centres are comparable too. Taking into account the long radiative lifetime and strong non-radiative decay channel, it is unlikely that the GR1 and 3H centres could serve as efficient single-photon emitters.

There is one more general disadvantage pertaining to all intrinsic optical centres. The intrinsic centres cannot be produced deterministically using the irradiation techniques. Indeed,

energetic particles damage statistically the diamond lattice along the path of their propagation and thus may produce point defects through the whole damaged volume. This means that neither the number nor the position of intrinsic point defects created even by irradiation with single low-energy particles can be controlled precisely.

#### 4.6. Optical centres for fibre optics

When talking about single-photon optical centres suitable for fibre optics communication systems, their spectra should be compared with those of transparency of glass fibre and sensitivity of silicon single-photon detectors. Figure 11(a) shows that the transparency window of a glass fibre has a sharp edge at 800 nm and the maximum transparency is achieved at a wavelength of 1300 and 1600 nm. None of the aforementioned centres emits in the desirable spectral range. However, all of them are still in the range of high sensitivity of silicon single-photon detectors.

An interesting alternative could be the 812 nm Xe-related centre, which emits photons at room temperature preferentially in ZPL at a wavelength of 812 nm with a width of 10 nm (figure 11(b)) [81, 82]. The single-photon emission of this centre has not been measured yet. However, imaging of individual Xe-centres has already been demonstrated [83]. Another IR impurity-related centre, which should be tested for single-photon emission, is the 991.8 nm centre containing titanium [84] (figure 11(c)). The 998.1 nm centre, like most centres involving atoms of transition metal, has low electron–phonon interaction and emits mostly in its ZPL.

The absence of luminescence centres in diamond emitting in the infrared at a wavelength longer than 1000 nm has been discussed in [85, 86]. It was assumed that the reason for low efficiency of IR luminescence of optical centres diamond may be very high energy of diamond phonons. When the phonon energy becomes comparable with that of the electronic transition, the non-radiative decay of the excited states becomes strong, especially for centres with great electron–phonon coupling. Thus, the inefficiency of diamond in terms of the formation of optical centres working at the telecommunication wavelength has been considered as its natural limitation and it has been suggested that the search for effective IR luminescence centres in diamond might be in vain. However, it was rightly assumed that very compact defects containing multicharged ions of transition metal and/or rare earth elements may produce optical centres with very low electron–phonon coupling. These centres, consequently, could reveal high-luminescence efficiency even in the IR spectral range.

### 5. Application of optical centres in diamond single photon light-emitting diodes (LEDs)

All of the above mentioned optical centres were demonstrated as single-photon emitters in the regime of photoluminescence. However, it is a great advantage of a single-photon source when it is electrically driven. Electrical excitation allows, firstly, to avoid an intermediate photoexcitation step and, secondly, to design a single-photon source as a nano-optoelectronic device. Direct electrical excitation is a common feature of all of the light sources based on semiconductor structures. Many optical centres in diamond can be excited in electroluminescence [8]. So far the most efficient of them have been shown to be the H3 nitrogen-related centre, the 575 nm NV<sup>0</sup> nitrogen-related centre, the 738 nm silicon-related SiV centre and the 812 nm Xe-related centre (figure 11(b)). The NV<sup>-</sup> centre cannot be excited

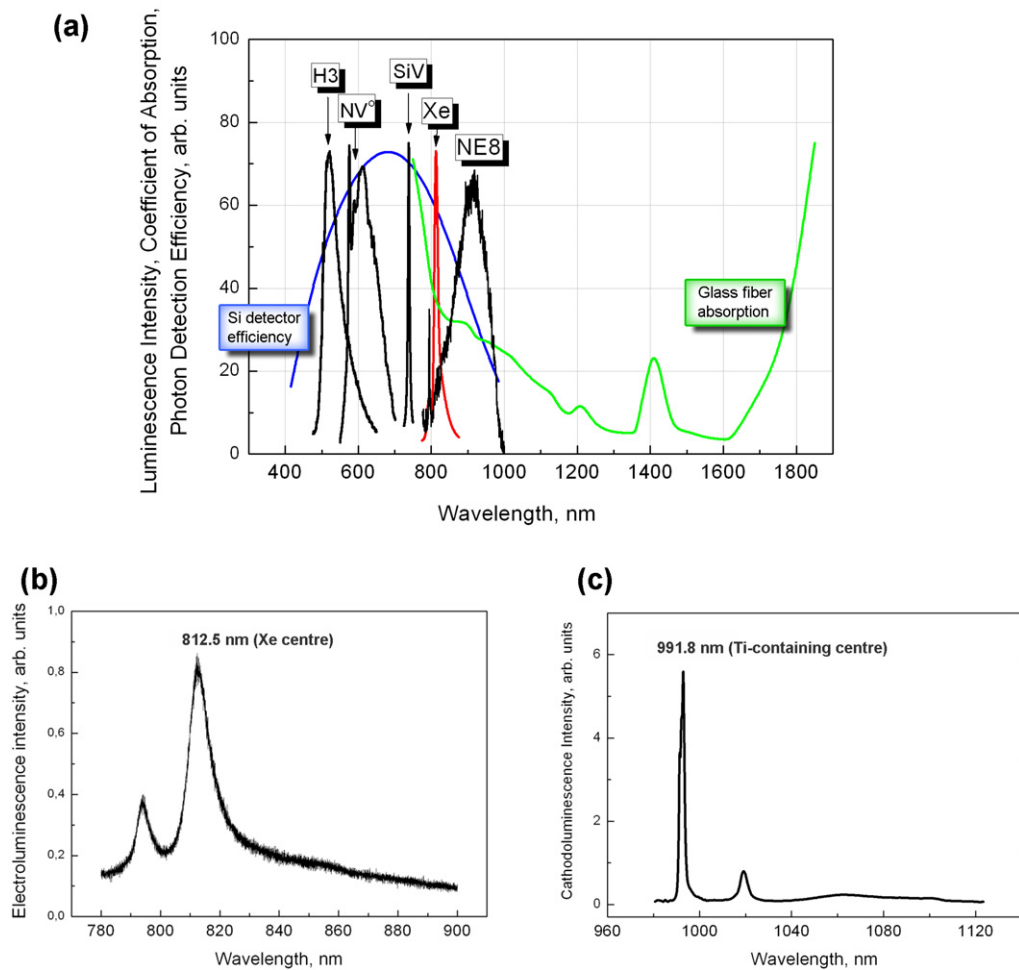


**Figure 11.** (a) Comparison of RT electroluminescence spectra of the H3 centre, NV<sup>0</sup> centre (575 nm centre), Si-V centre (all excited in diamond p-i-n LEDs), Xe-centre (excited in photoluminescence at 200 K) with the spectral efficiency of a commercial silicon photon detector (SPCM-AQR, [www.perkinelmer.com/opto](http://www.perkinelmer.com/opto)). (b) Room-temperature spectrum of electroluminescence of a p-i-n diamond diode activated with Xe-centre. (c) Cathodoluminescence spectrum of diamond implanted with Ti ions. The measurements were performed at liquid nitrogen temperature. Replotted from [84].

electrically [87]. It reveals no electro- or cathodo-luminescence and, hence, can be used exclusively in optically pumped photoluminescence systems.

Different diamond-based diodes capable of electroluminescence excitation of optical centres have been demonstrated so far: p-i-p, p-i-M, M-i-M and p-i-n. The p-i-n diodes made by B<sup>+</sup> (for p-type doping [88]) and Li<sup>+</sup> (for n-type doping [89]) ion implantation appear to be the most preferable devices because they show high performance [90]. In addition, the LEDs made by ion implantation are scalable down to the sub-micrometer level. When made on high-quality diamond substrates, diamond p-i-n diodes show low working voltage

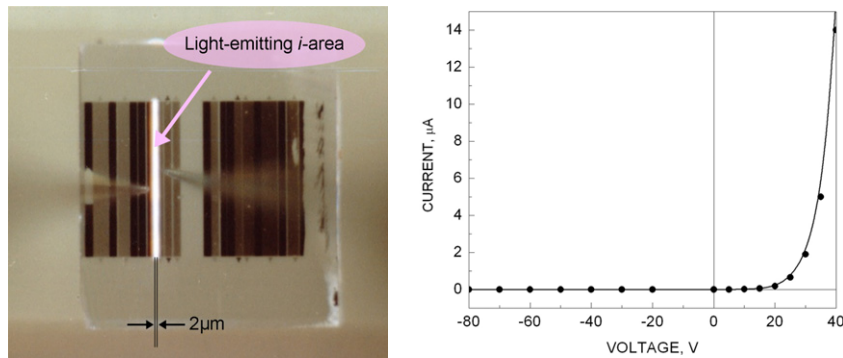


**Figure 12.** Emission of a diamond p-i-n LED with 2 μm i-area and its current-voltage characteristic. The i-area of the diode is activated with H3 and 575 nm centres. Detectable light emission starts at a forward voltage of 15 V as a pattern of many shining dots along the i-stripe. With a voltage increase, the electroluminescence uniformly covers the whole i-stripe. The picture shows the emission at a forward voltage of 40 V (courtesy of A A Melnikov).

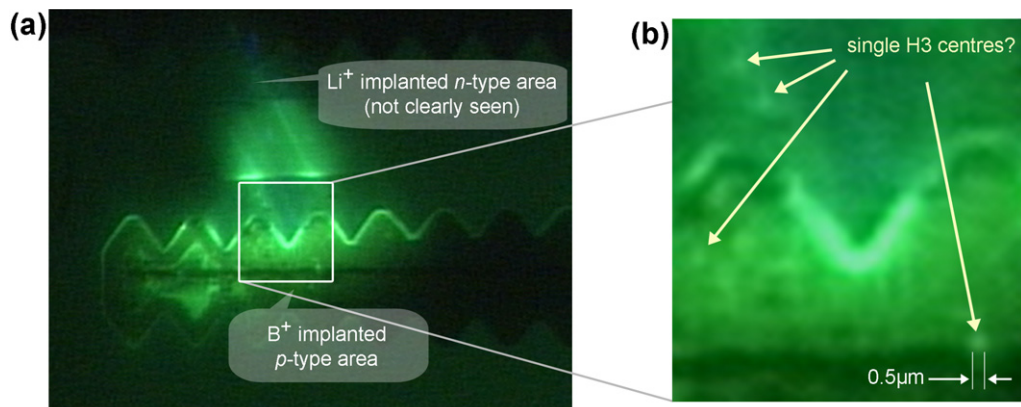


**Figure 13.** (a) Electroluminescence of a planar p-i-n micro-diode made on a low-nitrogen natural diamond substrate (forward bias 90 V, total current 60 μA). The emission is dominated by the H3 centres. The current flow and electroluminescence excitation over the diode area are highly non-uniform due to a non-homogeneity of nitrogen distribution, characteristic of natural diamonds. (b) In the regions with low electroluminescence, the emission breaks down into a spotty pattern, the smallest size of the spots being of 0.5 μm (resolution of optical microscope). These spots are believed to be the emission of small clusters and individual H3 centres.

(down to 5 V) and high external quantum efficiency. Figure 12 presents a photograph of a diamond p-i-n diode with a 2 μm wide i-area and its current voltage characteristic.

P-i-n diodes, the i-areas of which contain low concentration of optical centres, may exhibit at low currents an uneven dot-like distribution of electroluminescence (figure 13(a)). Such a dotted pattern is believed to originate from the discrete distribution of small clusters of optical centres as well as single optical centres (figure 13(b)).

## 6. Conclusion and outlook

The deterministic creation of a single-photon emitter with appropriate spectral and temporal parameters still remains one of the main challenges of quantum communication physics. However, recent developments in this field have brought us close to the realization of this task. Today we understand what a good single-photon source is and already have examples of such sources with parameters approaching the desirable ones. These sources are the luminescent active point defects in diamond. Unprecedented stability of diamond lattice provides the required structural stability of the defects, in terms of both photostability and temperature stability. Diamond possesses an enormous number of optically active defects with very broad range of spectral and temporal parameters. It is important that these defects can be artificially created as impurity atom clusters via doping. By now we know 27 impurity atoms that form over 100 optically active centres in diamond. They alone provide a broad spectrum of centres to choose from. However, the real engineering of optical centres with required parameters will come with development of multispecies doping. An example of dual doping of diamond with optically active He and N presented in [8] shows that co-doping may result in the creation of very different optical centres that cannot be achieved by monospecies doping alone. As the number of combinations of optically active species is almost unlimited, one can expect that the probability of creation of an optical centre with required parameters is really high.

It is crucial that impurity doping of diamond can be achieved by ion implantation. Today, the implantation with single ions is the only method of controllable fabrication of individual optical centres working as single-photon sources at room temperature. The achievements in the development of single-ion implantation techniques are very encouraging and they make the fabrication of individual optical centres in diamond and their predetermined assemblies at nanometre scale a reality.

The possibility of fabrication of the electrically driven single-photon sources is very important for practical applications because they could be made in as micro- and nano-optoelectronic devices compatible with existing microelectronic technology. Fortunately, diamond offers a good opportunity for fabrication of light-emitting diodes, which can excite electroluminescence of most of the known optical centres. Like the creation of the optical centres, the fabrication of diamond LEDs can be done by ion implantation using electrically active impurities. Employing well-developed nanobeam techniques, it is quite realistic to fabricate a diamond LED with a nanoscale size active i-area accommodating single optical centre. Such a nano-LED on diamond may appear a real prototype of a nano-optoelectronic single-photon source.

## Acknowledgments

We acknowledge the financial support of the Volkswagen Foundation and the State of North Rhine-Westphalia through the Research Department Integrity of Small-Scale Systems/High Temperature Materials. One of us, AZ, greatly appreciates the support of US army research office (grant no. 49658-EL-H).

## References

- [1] Kurtsiefer C, Mayer S, Zarda P and Weinfurter H 2000 Stable solid-state source of single photons *Phys. Rev. Lett.* **85** 290–3
- [2] Wang C, Kurtsiefer C, Weinfurter H and Burchard B 2006 Single photon emission from SiV centres in diamond produced by ion implantation *J. Phys. B: At. Mol. Opt. Phys.* **39** 37–41
- [3] Simpson D A, Ampem-Lassen E, Gibson B C, Trpkovski S, Hossain F M, Huntington S T, Greentree A D, Hollenberg L C L and Prawer S 2009 A highly efficient two level diamond based single photon source *Appl. Phys. Lett.* **94** 203107
- [4] Aharonovich I, Castelletto S, Simpson D A, Stacey A, McCallum J, Greentree A D and Prawer S 2009 Two-level ultrabright single photon emission from diamond nanocrystals *Nano Lett.* **9** 3191–5
- [5] Gaebel T, Popa I, Gruber A, Domhan M, Jelezko F and Wrachtrup J 2004 Stable single-photon source in the near infrared *New J. Phys.* **6** 98
- [6] Pezzagna S, Wildanger D, Mazarov P, Wieck A D, Sarov Y, Rangelow I, Naydenov B, Jelezko F, Hell S W and Meijer J 2010 Nanoscale engineering and optical addressing of single spins in diamond *Small* **6** 2117–21
- [7] Toyli D M, Weis C D, Fuchs G D, Schenkel T and Awschalom D 2010 Chip-scale nanofabrication of single spins and spin arrays in diamond *Nano Lett.* **10** 3168–72
- [8] Zaitsev A M 2001 *Optical Properties of Diamond* (Berlin: Springer)
- [9] Ziegler J 2008 The stopping range of ions in matter, SRIM-2008 Online at: <http://srim.org>
- [10] Williams J S and Elliman R G 1989 *Ion Beams for Material Analysis* (Australia: Academic Press)
- [11] Hobler G 1996 Critical angles and low-energy limits to ion channelling in silicon *Radiat. Eff. Defects Solids* **139** 21–85
- [12] Derry T E, Fearick R W and Sellschop J P F 1982 Ion channelling in natural diamond. II. Critical angles *Phys. Rev. B* **26** 17–25
- [13] Turner N L, Current M I, Smith T C, Crane D and Simonton R 1985 Avoidance of planar channeling effects in Si(100) *Proc. SPIE* **530** 55–69
- [14] Allers L, Collins A T and Hiscock J 1998 The annealing of interstitial-related optical centres in type II natural and CVD diamond *Diam. Relat. Mater.* **7** 228–32
- [15] Alekseev A G, Amosov V N, Krasil'nikov A V, Tugarinov S N, Frunze V V and Tsutskikh A Y 2000 Transformation of GR1 defects in annealed natural type IIa diamonds *Tech. Phys. Lett.* **26** 496–8
- [16] Gippius A A, Khmel'nitskiy R A, Dravin V A and Tkachenko S D 1999 Formation and characterization of graphitized layers in ion-implanted diamond *Diam. Relat. Mater.* **8** 1631–4
- [17] Santori C, Barclay P E, Fu K-M C and Beausoleil R G 2009 Vertical distribution of nitrogen-vacancy centers in diamond formed by ion implantation and annealing *Phys. Rev. B* **79** 125313
- [18] Iakoubovskii K and Adriaenssens G J 2001 Trapping of vacancies by defects in diamond *J. Phys.: Condens. Matter* **13** 6015–8
- [19] Laikhtman A, Lafosse A, Le Coat Y, Azria R and Hoffman A 2004 Interaction of water vapour with bare and hydrogenated diamond film surfaces *Surf. Sci.* **551** 99–105
- [20] Manelli O, Corni S and Righi M C 2010 Water adsorption on native and hydrogenated diamond (001) surfaces *J. Phys. Chem. C* **114** 7045–53
- [21] Fu K-M C, Santori C, Barclay P E and Beausoleil R G 2010 Conversion of neutral nitrogen-vacancy centers to negatively charged nitrogen-vacancy centers through selective oxidation *Appl. Phys. Lett.* **96** 121907
- [22] Rondin L *et al* 2010 Surface-induced charge state conversion of nitrogen-vacancy defects in nanodiamonds *Phys. Rev. B* **82** 115449
- [23] Hauf M V *et al* 2011 Chemical control of the charge state of nitrogen-vacancy centers in diamond *Phys. Rev. B* **83** 081304
- [24] Naydenov B, Reinhard F, Lämmle A, Richter V, Kalish R, D'Haenens-Johansson U F S, Newton M, Jelezko F and Wrachtrup J 2010 Increasing the coherence time of single electron spins in diamond by high-temperature annealing *Appl. Phys. Lett.* **97** 242511

- [25] Tkachev V D, Mudryi A V and Minarev N S 1984 Noble gas atoms as chemical impurities in silicon *Phys. Status Solidi* **81** 313–21
- [26] Rittweger E, Han K Y, Irvine S E, Eggeling C and Hell S W 2009 STED microscopy reveals crystal colour centres with nanometric resolution *Nat. Photonics* **3** 144–7
- [27] Gurudev Dutt, Childress L, Jiang L, Togan E, Maze J, Jelezko F, Zibrov A S, Hemmer P R and Lukin M D 2007 Quantum register based on individual electronic and nuclear spin qubits in diamond *Science* **316** 1312–6
- [28] Neumann P, Mizuochi N, Rempp F, Hemmer P, Watanabe H, Yamasaki S, Jacques V, Gaebel T, Jelezko F and Wrachtrup J 2008 Multipartite entanglement among single spins in diamond *Science* **320** 1326–9
- [29] Neumann P *et al* 2010 Quantum register based on coupled electron spins in a room-temperature solid *Nat. Phys.* **6** 249–53
- [30] Maze J R *et al* Nanoscale magnetic sensing with an individual electronic spin in diamond *Nature* **455** 644–7
- [31] Balasubramanian G *et al* 2008 Nanoscale imaging magnetometry with diamond spins under ambient conditions *Nature* **455** 648–51
- [32] Balasubramanian G *et al* 2009 Ultralong spin coherence time in isotopically engineered diamond *Nat. Mater.* **8** 383–7
- [33] Fu C-C, Lee H-Y, Chen K, Lim T-S, Wu H-Y, Lin P-K, Wei P-K, Tsao P-H, Chang H-C and Fann W 2007 Characterization and application of single fluorescent nanodiamonds as cellular biomarkers *Proc. Natl Acad. Sci. USA* **104** 727–32
- [34] Neugart F, Zappe A, Jelezko F, Tietz C, Boudou J-P, Krueger A and Wrachtrup J 2007 Dynamics of diamond nanoparticles in solution and cells *Nano Lett.* **7** 3588–91
- [35] Meijer J and Stephan A 2002 Prospects of ion projection techniques for maskless implantation at high ion energies *Nucl. Instrum. Methods B* **188** 9–17
- [36] Meijer J, Burchard B, Ivanova K, Volland B E, Rangelow I W, Rüb M and Deboy G 2004 High energy ion projection for deep ion implantation as a low cost high throughput alternative for subsequent epitaxy process *J. Vac. Sci. Technol. B* **22** 152–7
- [37] Meijer J, Burchard B, Domhan M, Wittmann C, Gaebel T, Popa I, Jelezko F and Wrachtrup J 2005 Generation of single color centers by focused nitrogen implantation *Appl. Phys. Lett.* **87** 261909
- [38] Spinicelli P *et al* 2011 Engineered arrays of NV color centers in diamond based on implantation of CN-molecules through nanoapertures *New J. Phys.* **13** 025014
- [39] Meijer J *et al* 2008 Towards the implanting of ions and positioning of nanoparticles with nm spatial resolution *Appl. Phys. A* **91** 567–71
- [40] Li J, Stein D, McMullan C, Branton D, Aziz M J and Golovchenko J A 2001 Ion-beam sculpting at nanometre length scales *Nature* **412** 166–9
- [41] Schenkel T, Persaud A, Park S J, Meijer J, Kingsley J R, McDonald J W, Holder J P, Bokor J and Schneider D H 2002 Single ion implantation for solid state quantum computer development *J. Vac. Sci. Technol. B* **20** 2819–23
- [42] Jamieson D N *et al* 2005 Controlled shallow single-ion implantation in silicon using an active substrate for sub-20-keV ions *Appl. Phys. Lett.* **86** 202101
- [43] Meijer J *et al* 2006 Concepts of deterministic single ion doping with sub-nm spatial resolution *Appl. Phys. A* **83** 321–27
- [44] Schnitzler W, Linke N M, Fickler R, Meijer J, Schmidt-Kaler F and Singer K 2009 Deterministic ultracold ion source targeting the Heisenberg limit *Phys. Rev. Lett.* **102** 070501
- [45] Schnitzler W, Jacob G, Fickler R, Schmidt-Kaler F and Singer K 2010 Focusing a deterministic single-ion beam *New J. Phys.* **12** 065023
- [46] Hell S W 2003 Toward fluorescence nanoscopy *Nat. Biotechnol.* **21** 1347–55
- [47] Hell S W and Wichmann J 1994 Breaking the diffraction resolution limit by stimulated emission *Opt. Lett.* **19** 780–2
- [48] Hell S W and Kroug M 1995 Ground-state depletion fluorescence microscopy, a concept for breaking the diffraction resolution limit *Appl. Phys. B* **60** 495–7

- [49] Bretschneider S, Eggeling C and Hell S W 2007 Breaking the diffraction barrier in fluorescence microscopy by optical shelving *Phys. Rev. Lett.* **98** 218103
- [50] Han K Y, Kim S K, Eggeling C and Hell S W 2010 Metastable dark states enable ground state depletion microscopy of nitrogen vacancy centers in diamond with diffraction-unlimited resolution *Nano Lett.* **10** 3199–203
- [51] Rittweger E, Wildanger D and Hell S W 2009 Far-field fluorescence nanoscopy of diamond color centers by ground state depletion *Euro. Phys. Lett.* **86** 14001
- [52] Maurer P C *et al* 2010 Far-field optical imaging and manipulation of individual spins with nanoscale resolution *Nat. Phys.* **6** 912–8
- [53] Orwa J O, Greentree A D, Aharonovich I, Alves A D C, Van Donkelaar J, Stacey A and Prawer S 2010 Fabrication of single optical centres in diamond—a review *J. Lumin.* **130** 1646–54
- [54] Jacques V, Neumann P, Beck J, Markham M, Twitchen D, Meijer J, Kaiser F, Balasubramanian G, Jelezko F and Wrachtrup J 2009 Dynamic polarization of single nuclear spins by optical pumping of nitrogen-vacancy color centers in diamond at room temperature *Phys. Rev. Lett.* **102** 5
- [55] Neumann P, Beck J, Steiner M, Rempp F, Fedder H, Hemmer P R, Wrachtrup J and Jelezko F 2010 Single-shot readout of a single nuclear spin *Science* **329** 542–4
- [56] Beveratos A, Brouri R, Gacoin T, Poizat J-P and Grangier P 2001 Nonclassical radiation from diamond nanocrystals *Phys. Rev. A* **64** 061802
- [57] Pezzagna S, Naydenov B, Jelezko F, Wrachtrup J and Meijer J 2010 Creation efficiency of nitrogen-vacancy centres in diamond *New J. Phys.* **12** 065017
- [58] Naydenov B, Richter V, Beck J, Steiner M, Neumann P, Balasubramanian G, Achard J, Jelezko F, Wrachtrup J and Kalish R 2010 Enhanced generation of single optically active spins in diamond by ion implantation *Appl. Phys. Lett.* **96** 163108
- [59] Collins A T 2002 The Fermi level in diamond *J. Phys.: Condens. Matter* **14** 3743–50
- [60] Vlasov I I, Barnard A S, Ralchenko V G, Lebedev O I, Kanzyuba M V, Saveliev A V, Konov V I and Goovaerts E 2009 Nanodiamond photoemitters based on strong narrow-band luminescence from silicon-vacancy defects *Adv. Mater.* **21** 808–12
- [61] Basov A A, Rahn M, Pärns M, Vlasov I I, Sildos I, Bolshakov A P, Golubev V G and Ralchenko V G 2009 Spatial localization of Si-vacancy photoluminescent centers in a thin CVD nanodiamond film *Phys. Status Solidi* **206** 2009–11
- [62] Rabeau J R, Chin Y L and Prawer S 2005 Fabrication of single nickel-nitrogen defects in diamond by chemical vapor deposition *Appl. Phys. Lett.* **86** 131926
- [63] Wu E, Jacques V, Zeng H, Grangier P, Treussart F and Roch J-F 2006 Narrow-band single-photon emission in the near infrared for quantum key distribution *Opt. Express* **14** 1296–303
- [64] Nadolinny V A, Yelissev A P, Baker J M, Newton M E, Twitchen D J, Lawson S C, Yuryeva O P and Feigelson B N 1999 A study of  $^{13}\text{C}$  hyperfine structure in the EPR of nickel–nitrogen-containing centres in diamond and correlation with their optical properties *J. Phys.: Condens. Matter* **11** 7357–76
- [65] Brout R and Visscher W 1962 Suggested experiment on approximate localized modes in crystals *Phys. Rev. Lett.* **9** 54
- [66] Zaitsev A M 2000 Vibronic spectra of impurity-related optical centers in diamond *Phys. Rev. B* **61** 12909
- [67] Gaillou E, Post J E, Bassim N D, Zaitsev A M, Rose T, Fries M D, Stroud R M, Steele A and Butler J E 2010 Spectroscopic and microscopic characterizations of color lamellae in natural pink diamonds *Diam. Relat. Mater.* **19** 1207–20
- [68] Wolfer M, Kriele A, Williams O A, Obloh H, Leancu C-C and Nebel C E 2009 Nickel doping of nitrogen enriched CVD-diamond for the production of single photon emitters *Phys. Status Solidi a* **206** 2012–5
- [69] Marshall G D, Gaebel T, Matthews J C F, Enderlein J, O'Brien J L and Rabeau J R 2011 Coherence properties of a single dipole emitter in diamond *New J. Phys.* accepted
- [70] Yelissev A P 2010 personal communication

- [71] Aharonovich I, Zhou C, Stacey A, Treussart F, Roch J-F and Praver S 2009 Formation of color centers in nanodiamonds by plasma assisted diffusion of impurities from the growth substrate *Appl. Phys. Lett.* **93** 243112
- [72] Aharonovich I, Zhou C, Stacey A, Orwa J, Castelletto S, Simpson D, Greentree A D, Treussart F, Roch J-F and Praver S 2009 Enhanced single-photon emission in the near infrared from a diamond color center *Phys. Rev. B* **79** 235316
- [73] Steinmetz D, Neu E, Meijer J, Bolse W and Becher C 2010 Single photon emitters based on Ni/Si related defects in single crystalline diamond arXiv:1007.0202
- [74] Aharonovich I, Castelletto S, Johnson B C, McCallum J C, Simpson D A, Greentree A D and Praver S 2010 Chromium single-photon emitters in diamond fabricated by ion implantation *Phys. Rev. B* **81** 121201
- [75] Siyushev P *et al* 2009 Low-temperature optical characterization of a near-infrared single-photon emitter in nanodiamonds *New J. Phys.* **11** 113029
- [76] Naydenov B, Kolesov R, Batalov A, Meijer J, Pezzagna S, Rogalla D, Jelezko F and Wrachtrup J 2009 Engineering single photon emitters by ion implantation in diamond *Appl. Phys. Lett.* **95** 181109
- [77] Clark C D and Norris C A 1971 Photoluminescence associated with the 1.673, 1.944 and 2.498 eV centres in diamond *J. Phys. C: Solid State Phys.* **4** 2223–9
- [78] Collins A T, Szechi J and Tavender S 1988 Resonant excitation of the GR centre in diamond *J. Phys. C: Solid State Phys.* **21** L161–64
- [79] Bilodeau T G, Doverspike K, Strom U, Freitas J A and Rameshan R 1993 Calorimetric absorption-spectroscopy and photoluminescence study of defects in diamond *Diam. Relat. Mater.* **2** 699
- [80] De Weert F, Collins A T, Zugik M and Connor A 2005 Sub-threshold excitation of luminescence of defects in diamond *J. Phys.: Condens. Matter* **17** 8005–15
- [81] Zaitsev A M, Bergman A A, Gorokhovskiy A A and Huang M 2006 Diamond light emitting diode activated with Xe optical centres *Phys. Status Solidi a* **203** 638–42
- [82] Bergman A A, Zaitsev A M and Gorokhovskiy A A 2007 Polarization of luminescence and site symmetry of the Xe center in diamond *J. Lumin.* **125** 92–6
- [83] Gorokhovskiy A A 2008 personal communication
- [84] Gippius A A and Collins A T 1993 Defect induced structure of the 998.1 nm titanium luminescence line in diamond *Solid State Comm.* **88** 637–8
- [85] Rogers L J, Armstrong S, Sellars M J and Manson N B 2008 Infrared emission of the NV centers in diamond: Zeeman and uniaxial stress studies *New J. Phys.* **10** 103024
- [86] Rogers L 2010 How far into the infrared can a color centre in diamond emit *Phys. Procedia* **3** 1557–61
- [87] Field J E 1992 *The Properties of Natural and Synthetic Diamond* (London: Academic)
- [88] Vogel T, Meijer J and Zaitsev A 2004 Highly effective p-type doping of diamond by MeV-ion implantation of boron *Diam. Relat. Mater.* **13** 1822–5
- [89] Chernyshev V A, Meijer J, Grambole D, Hermann F, Dagkaldiran Ü and Wieck A D 2008 n-Type diamond produced by MeV lithium implantation in channelling direction *Diam. Relat. Mater.* **17** 1933–5
- [90] Melnikov A A, Denisenko A V, Zaitsev A M, Shulenkov A, Varichenko V S, Filipp A R, Dravin V A, Kanda H and Fahrner W R 1998 Electrical and optical properties of light emitting p–i–n diodes on diamond *J. Appl. Phys.* **84** 6127